

Microwave photonic integrator based on a multichannel fiber Bragg grating

JIEJUN ZHANG AND JIANPING YAO*

Microwave Photonics Research Laboratory, University of Ottawa, 800 King Edward Avenue, Ontario K1N 6N5, Canada

*Corresponding author: jpyao@uottawa.ca

Received 23 September 2015; revised 18 November 2015; accepted 19 November 2015; posted 24 November 2015 (Doc. ID 250706); published 7 January 2016

We propose and experimentally demonstrate a microwave photonic integrator based on a multichannel fiber Bragg grating (FBG) working in conjunction with a dispersion compensating fiber (DCF) to provide a step group delay response with no in-channel dispersion-related distortion. The multichannel FBG is designed based on the spectral Talbot effect, which provides a large group delay dispersion (GDD) within each channel. A step group delay response can then be achieved by cascading the multichannel FBG with a DCF having a GDD opposite the in-channel GDD. An optical comb, with each comb line located at the center of each channel of the FBG, is modulated by a microwave signal to be integrated. At the output of the DCF, multiple time-delayed replicas of the optical signal, with equal time delay spacing are obtained and are detected and summed at a photodetector (PD). The entire operation is equivalent to the integration of the input microwave signal. For a multichannel FBG with an in-channel GDD of 730 ps/nm and a DCF with an opposite GDD, an integrator with a bandwidth of 2.9 GHz and an integration time of 7 ns is demonstrated. © 2016 Optical Society of America

OCIS codes: (070.1170) Analog optical signal processing; (060.3738) Fiber Bragg gratings, photosensitivity.

<http://dx.doi.org/10.1364/OL.41.000273>

Photonic signal processing is considered to be a solution to alleviating the bandwidth bottleneck of electronic signal processing and has applications where high speed and wideband signal processing are needed. Among the numerous signal processing functions, a temporal integrator is a fundamental building block that has been widely investigated in the past few years. A photonic integrator, used to implement the temporal integration of an electronic signal, can operate at a much higher speed and wider bandwidth, compared to an electronic integrator. So far, photonic integrators have been demonstrated using a fiber Bragg grating (FBG) [1–4], a microring resonator [5,6], an active Fabry–Perot filter [7], or an optical dispersive device [8–11]. For example, a photonic integrator was demonstrated with a weak uniform FBG [1]. For an FBG with a physical length of 5 mm, the integration time window was only around

50 ps, which is very small. To increase the integration time window, two superimposed FBGs fabricated in an Er–Yb co-doped optical fiber were used to form an active optical resonator [2]. A temporal window of 2.9 ns was demonstrated. In [3,4], a high-order photonic integrator using a specially designed FBG with its spectral response corresponding to the spectrum of a higher order integrator was demonstrated. A photonic integrator can also be implemented using a microring resonator [5,6]. In [5], a passive microring resonator on a silica platform was used to perform the integration of an input signal with a time feature as fast as 8 ps. An integration time window of 800 ps was achieved. To realize an even longer integration time window, a photonic integrator based on an active InP–InGaAsP integrated ring resonator was proposed [6]. Due to the active nature of the ring resonator, the Q -factor can be controlled to be large, which leads to a significantly increased integration time of 6.3 ns. However, the larger diameter of the active ring resonator, compared to that of a passive ring resonator [5], resulted in a reduced bandwidth of 15 GHz. In [7], an active Fabry–Perot filter incorporating a semiconductor optical amplifier (SOA) was proposed as a photonic integrator with a simulated integration time window of 160 ns and an operation bandwidth of 180 GHz. However, in an experimental implementation, the integration time window and the operation bandwidth may be smaller since the SOA may not operate in conditions as ideal as assumed in the simulations. A photonic integrator can also be realized with an optical dispersive device, such as a dispersion compensating fiber (DCF) or simply a single-mode fiber (SMF). Due to their passive nature, such integrators are simpler and have smaller noise figures. For example, an integrator was demonstrated using a length of SMF as a dispersive device to generate time-delayed replicas of a signal that was carried by an incoherent broadband source with a rectangular spectrum. The time-delayed replicas are summed at a photodetector (PD). The entire operation is equivalent to an integrator [8]. The integrator in [8] allows the processing of an electrical signal with a time feature as fast as 7 ps, but the integration time window of 0.5 ns was small. To increase the integration time window, in [9], an integrator consisting of a low-speed integrator and a high-speed integrator that are cascaded was proposed. The integration time window was increased to 4 ns. However, for both integrators in [8,9],

since an incoherent light source was used, the signal-to-noise ratio (SNR) for the output signal was poor. To increase the SNR, in [10], the incoherent source was replaced by a multi-wavelength laser source. Again, an integration time window of 1.24 ns and a bandwidth of 36.8 GHz were achieved. In [11], a photonic system reconfigured as either an integrator or a differentiator, in which a multiwavelength laser source and 5 km SMF were used, was demonstrated. However, the integration time window was only 280 ps. Compared to an integrator based on an FBG or a resonator, an integrator based on a dispersive device can reach an extremely long integration time window simply by having the group delay dispersion (GDD) of the dispersive device increased. However, a large GDD may lead to significant distortions in a wideband input signal, such as temporal stretching of the signal [8] or a dispersion-induced power penalty to the signal [12].

In this Letter, we demonstrate a microwave photonic integrator based on a specially designed optical delay line consisting of a multichannel FBG and a DCF, to generate multiple time-delayed replicas of an input signal, without causing in-channel dispersion-induced distortions. The key component in the integrator is the multichannel FBG, which is working in conjunction with the DCF to form a delay line with a step GDD. Since there is no in-channel GDD, in-channel dispersion-induced distortions that exist in a simple delay-line-based integrator are avoided. In the system, an optical comb, with each of the comb lines located at the center of a channel of the FBG, is used as the optical carrier, which is modulated by an input microwave signal to be integrated. At the output of the delay line, multiple precisely time-delayed replicas of the input microwave signal are obtained, which are detected and summed at a PD. The entire operation is equivalent to an integrator.

The integration of an input microwave signal $x(t)$ can be mathematically expressed as

$$y(t) = \int_{t_0}^t x(t') dt', \quad (1)$$

which can be approximated as the summation of the time-delayed replicas in a discrete form,

$$y(m) = \sum_{n=0}^{m-1} x(t_0 + n\Delta t)\Delta t, \quad (2)$$

where n and m are integers, and Δt is the discrete time step. It is discussed in [8] that when Δt is smaller than the fastest time feature of the input signal $x(t)$, Eq. (1) can be well approximated by Eq. (2). The relationship between m and t is given by $t = m\Delta t$. It can be seen that the integration of an electrical signal can be realized by generating the time-delayed replicas of the analog signal $x(t)$ and summing the replicas. In photonics, a straightforward way to produce time-delayed replicas is to modulate the electrical signal on multiple optical carriers and allow the modulated optical carriers to experience different time delays in a dispersive delay line [10]. However, for wideband electrical signal integration, the GDD of the delay line may also change the phase relationship within the spectrum of the signal, which may cause significant distortions to the integrated output. An ideal optical delay line should provide different time delays to different optical carriers but no GDD to the time-delayed signals. A solution is to use an optical fiber delay line with a step group delay response.

The principle of using an optical delay line with a step group delay response to perform the integration of an electrical

rectangular waveform is illustrated in Fig. 1. First, the signal to be integrated is modulated on the comb lines of an optical comb, which is then sent to a specially designed optical delay line. The optical delay line has a step group delay response with a fixed time delay difference between adjacent channels, which is Δt , and no GDD within each channel. The comb lines are located at the centers of the channels, such that even if a broadband signal is modulated on the comb lines, the signal will not suffer from any dispersion-related distortions when traveling through the optical delay line. At the output of the optical delay line, multiple time-delayed replicas will be achieved with a time delay difference of Δt . The time-delayed replicas are then detected and summed at a PD. A profile proportional to the integration of the input signal within the integration time window of T is then achieved at the output of the PD.

Figure 2 presents a comparison by simulation between two integrators, one using a photonic delay line with a step group delay response and one using a photonic delay line with a linear group delay response. In the simulation, a Gaussian pulse with a temporal width of 40 ps is used as the input signal. The linear GDD is 730 ps/nm. The step group delay provides a time delay difference of 1 ps between adjacent channels, and a total of 200 channels are used in the simulation. As can be seen, when using a photonic delay line with a linear group delay response, the input signal suffers from strong distortions due to the linear GDD. The integrated output waveform is very different from that of an ideal integrator. However, when a photonic link with step group delay response is used, the time-delayed signals are free from dispersion-related distortions, and accurate integration is achieved within a time window. A photonic delay line with a step group delay response is especially important for the integration of a signal with a large bandwidth.

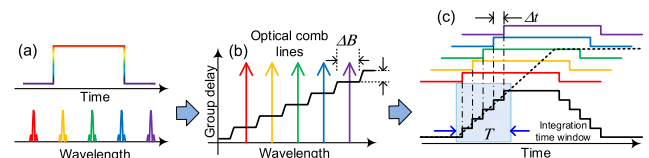


Fig. 1. Principle of an integrator based on an optical delay line with a step group delay response: (a) the time and wavelength domain representation of the signal to be integrated, which is a rectangular waveform modulated on the comb lines of an optical comb; (b) the step group delay response of the optical delay line (black line), with the comb lines located at the centers of the channels (illustrated as arrows in different colors); (c) the generated time-delayed replicas and their summation. The black dotted line represents the ideal integration result, and the black solid line shows the output of a practical integrator with an integration time window of T .

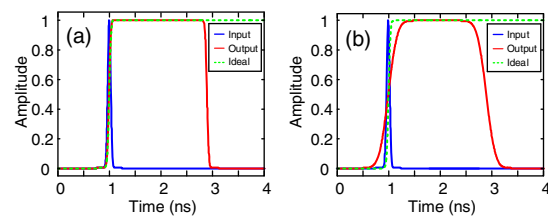


Fig. 2. Comparison of a microwave photonic integrator based on an optical delay line with (a) a step group delay response and (b) a linear group delay response.

There are two factors that limit the bandwidth of the proposed integrator. First, as shown in Fig. 1(b), each step in the group delay response has a bandwidth denoted by ΔB . The bandwidth of the input signal must be smaller than $\Delta B/2$ if double-sideband modulation is used. Otherwise, the input signal may suffer from dispersion-related distortions. Then, as indicated by Eq. (2), the bandwidth of the input signal must also be smaller than $1/\Delta t$, so that the summation of the time-delayed replicas will precisely represent the integration of the original signal [8]. In our case, ΔB is significantly larger than $1/\Delta t$, hence the bandwidth limit of the integrator is $1/\Delta t$. It should be noted that the bandwidth of the integrator is also limited by the optoelectronic devices used in the system, such as the electro-optic modulator and the PD.

The integration time window, on the other hand, can be easily seen from Fig. 1, which is given by

$$T = (N - 1) \cdot \Delta t, \quad (3)$$

where N is the number of the optical comb lines. The time-bandwidth product of the integrator is roughly given by $(N - 1)$. It can be seen that by using an optical comb with a large number of comb lines and a multichannel FBG with more channels, an integrator with a large time-bandwidth product can be achieved.

Figure 3 shows the schematic of the proposed microwave photonic integrator. A broadband source, a spectral shaper, and an erbium-doped fiber amplifier (EDFA) are used to generate an optical comb. The broadband source is the amplified spontaneous emission (ASE) of an EDFA. The spectral shaper has a comb-like transmission spectrum, thus an optical comb is generated at its output, which is then amplified by another EDFA. The optical comb is directed to a Mach-Zehnder modulator (MZM), which is biased in the linear modulation region but slightly lowered toward the minimum transmission point to reduce the optical power to the PD, to reduce the shot noise at the PD. A microwave signal generated by an electrical arbitrary waveform generator (AWG) is modulated to the optical comb lines at the MZM. The optical signal at the output of the MZM is sent to a multichannel FBG, where it is then reflected and directed to a DCF via an optical circulator. The linear dispersion within each channel is canceled by the opposite dispersion of the DCF. At the output of the DCF, multiple time-delayed replicas with no dispersion-related distortions are obtained and are applied to a PD. The group delay response of the multichannel FBG and that of the DCF are illustrated in Fig. 3. The multichannel FBG is designed to have a fixed in-channel GDD and small or no group delay difference between the channels. The in-channel GDD is then canceled by the opposite GDD of the DCF. The cascading of the multichannel FBG and the DCF provides the delay line with a step group delay, as shown in Fig. 1(b).

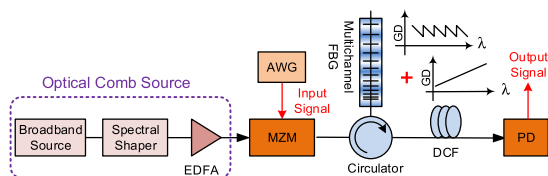


Fig. 3. Schematic of the proposed microwave photonic integrator. EDFA, erbium-doped fiber amplifier; AWG, arbitrary waveform generator; MZM, Mach-Zehnder modulator; DCF, dispersion compensating fiber; PD, photodetector; GD, group delay. Insets show the spectral group delay responses of the multichannel FBG and DCF.

The key device in the system is the multichannel FBG, which is designed, based on the spectral Talbot effect [13,14], by spatially sampling a chirped FBG. The refractive index modulation period along a linearly chirped FBG before sampling can be expressed as $\Lambda(z) = \Lambda + Cz$, where C and Λ are the chirp coefficient and the grating period, respectively. For simplicity, we choose a design where no phase shift is introduced between the channels of the multichannel FBG, and the sampling period is fixed. The relationship between the sampling period P , the FBG chirp coefficient C , and the in-channel chirp rate induced by the spectral Talbot effect C_0 is given by [15]

$$P = \frac{\Lambda}{\sqrt{C - C_0}}. \quad (4)$$

The chirp rate determines the in-channel GDD of the multichannel FBG by $d_\rho = 1/(vC_0)$, where v is the light velocity in vacuum. A multichannel response can be achieved with a channel spacing given by

$$\Delta\lambda = \frac{2n\Lambda^2}{P}, \quad (5)$$

where n is the refractive index of fiber. By cascading the multichannel FBG with a dispersive element having an opposite GDD of $-d_\rho$, the in-channel GDD will be fully canceled, with a time delay difference between adjacent channels of $\Delta T = \Delta\lambda d_\rho$.

An experiment based on the setup shown in Fig. 3 was performed. The broadband source, which is an EDFA with no input signal, generates an ASE light that covers the C band. The spectral shaper with a comb-like transmission spectrum is implemented by a programmable optical filter (Finisar 4000S) with 19 comb lines centered at 1554.82 nm and spaced by 0.471 nm. The AWG (Tektronix AWG7102) generates an electrical waveform to be integrated, which is then modulated to the optical comb lines at a 10 GHz MZM (JDSU OC-192).

The multichannel FBG is fabricated using a phase mask with UV illumination at 244 nm. The phase mask has a length of 5 cm and a linearly varying period from 1067.7 to 1076.1 nm. Note that the refraction index modulation period of the fabricated FBG is half of that of the phase mask. The spatial sampling period is chosen to be 1.9 mm with a duty cycle of 0.15. According to Eqs. (4) and (5), the in-channel GDD and the channel spacing can be calculated to be 700 ps/nm and 0.438 nm, respectively. The measured spectral response of the multichannel FBG is shown in Fig. 4. It can be seen that the in-channel GDD is 730 ps/nm and the channel spacing is 0.471 nm, which agree well with the theoretical values. The DCF has a GDD of -752 ps/nm, which cancels the in-channel GDD of the multichannel FBG, thus the electrical signal modulated on each comb line will not suffer from any dispersion-induced distortions. The combined group delay response of the multichannel FBG and the DCF is shown in Fig. 4(c). A step group delay response with a time delay difference of around 343 ps between two adjacent channels can be seen clearly, which corresponds to an integrator with a bandwidth of 2.9 GHz. The time-delayed signals at the output of the DCF are applied to a 25 GHz PD (New Focus 1414), where detection and summation of the time-delayed signals are performed. An integrated electrical signal is obtained at the output of the PD, which is monitored by a real-time oscilloscope (Agilent DSO-X 93204A).

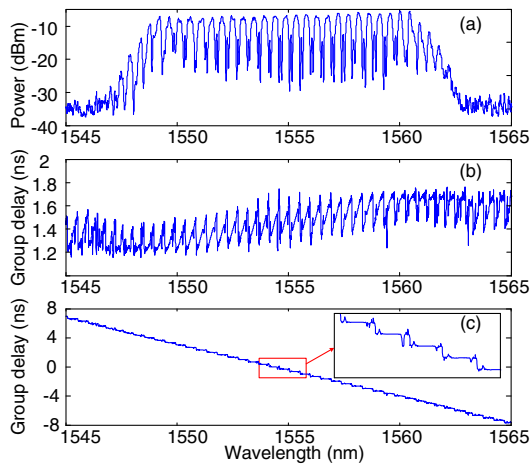


Fig. 4. (a) The measured reflection spectrum and (b) the group delay response of the multichannel FBG; (c) the combined group delay response of the multichannel FBG and the DCF.

Three different electrical waveforms are generated by the AWG to evaluate the operation of the integrator. The waveforms are an electrical pulse, a doublet pulse with a pulse separation of 3.5 ns, and a rectangular waveform with a width of 7 ns. The measured and simulated integration results are presented in Fig. 5. Figure 5(a) shows the input electrical signal that consists of a single electrical pulse and the corresponding integration result, which is a step function within the integration time window. It can be seen that an integration time window of 7 ns is achieved, indicating a time–bandwidth product of 20.3 for the integrator. Figure 5(b) shows the input electrical signal that consists of two electrical pulses separated by 3.5 ns (called a doublet pulse) and the corresponding integration result, which is a two-step function within the integration time window. Finally, an electrical rectangular waveform with a width of 7 ns, which is equal to the integration time window, is generated and used as an input signal. Figure 5 shows the integration result, which is a ramp function. All the results agree well with the theoretical predictions within the integration time window. If a delay line

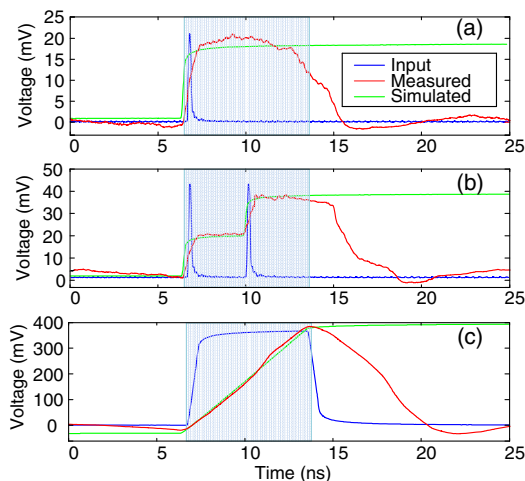


Fig. 5. Experimental and simulated integration results. The widths of the dashed boxes indicate the integration time windows. The input signal is (a) an electrical pulse, (b) a doublet pulse with a pulse spacing of 3.5 ns, and (c) a rectangular waveform with a gate width of 7 ns.

with a linear group delay response is used instead of the one with a step group response, the integration output may have some distortions for a wideband input signal. Since the AWG only has a sampling rate of 10 Gb/s, it cannot generate waveforms with a larger bandwidth, such as 25 GHz in Fig. 2, to make the dispersion-induced distortion sufficiently large to be observed. Note that the measured integration results are obtained based on 64 averaged samples. If the optical comb source used in the experiment is replaced by a multiwavelength laser source, the averaging operation is not needed due to the laser's strong optical power and low noise.

In conclusion, we have proposed and experimentally demonstrated a photonic integrator based on an optical delay line with a step group delay response. The key component in the system was the multichannel FBG, which was produced by spatially sampling a chirped FBG. By cascading a multichannel FBG with a DCF having an opposite dispersion within the channels, a delay line with a step group delay response was achieved. In the experiment, the multichannel FBG was fabricated with a channel spacing of 0.471 nm and an in-channel GDD of 730 ps/nm, and the DCF was selected to have a GDD of -752 ps/nm. Thus, the cascading of the multichannel FBG and the DCF provided a delay line with a fixed time delay of 344 ps between adjacent channels with no GDD in each channel. The electrical signal to be integrated was modulated to an optical comb source, of which the comb lines were located at the centers of the channels of the multichannel FBG. An integrator was then realized by propagating the modulated optical comb through the optical delay line to generate time-delayed replicas, which were detected and incoherently summed at the PD. In the experiment, three different microwave signals were used to test the operation of the integrator, indicating an integrator bandwidth of 2.9 GHz and an integration time window of 7 ns. The time–bandwidth product of the integrator was calculated to be 20.3, which is approximately equal to the number of channels used.

Funding. Natural Sciences and Engineering Research Council of Canada (NSERC); China Scholarship Council (201206160086).

REFERENCES

1. Y. Park, T.-J. Ahn, Y. Dai, J. Yao, and J. Azaña, *Opt. Express* **16**, 17817 (2008).
2. R. Slavik, Y. Park, N. Ayotte, S. Doucet, T.-J. Ahn, S. LaRochelle, and J. Azaña, *Opt. Express* **16**, 18202 (2008).
3. M. Asghari, C. Wang, J. Yao, and J. Azaña, *Opt. Lett.* **35**, 1191 (2010).
4. M. H. Asghari and J. Azaña, *J. Lightwave Technol.* **27**, 3888 (2009).
5. M. Ferrera, Y. Park, L. Razzari, B. E. Little, S. T. Chu, R. Morandotti, D. Moss, and J. Azaña, *Nat. Commun.* **1**, 1 (2010).
6. W. Liu, M. Li, R. S. Guzzon, E. J. Norberg, J. S. Parker, L. A. Coldren, and J. Yao, *J. Lightwave Technol.* **32**, 3654 (2014).
7. N. Huang, M. Li, R. Ashrafi, L. Wang, X. Wang, J. Azaña, and N. Zhu, *Opt. Express* **22**, 3105 (2014).
8. Y. Park and J. Azaña, *Opt. Lett.* **34**, 1156 (2009).
9. M. H. Asghari, Y. Park, and J. Azaña, *Opt. Lett.* **36**, 3557 (2011).
10. A. Malacarne, R. Ashrafi, M. Li, S. LaRochelle, J. Yao, and J. Azaña, *Opt. Lett.* **37**, 1355 (2012).
11. H. Jiang, L. Yan, J. Ye, W. Pan, B. Luo, and X. Zou, *IEEE Photon. Technol. Lett.* **25**, 2358 (2013).
12. J. Yao, *J. Lightwave Technol.* **27**, 314 (2009).
13. C. Wang, J. Azaña, and L. R. Chen, *Opt. Lett.* **29**, 1590 (2004).
14. Y. Dai and J. Yao, *J. Lightwave Technol.* **26**, 2513 (2008).
15. Y. Dai, X. Chen, X. Xu, C. Fan, and S. Xie, *IEEE Photon. Technol. Lett.* **17**, 1040 (2005).